Università degli studi di Udine

Structure of oleogels from κ-carrageenan templates as affected by supercritical-CO2-drying, freeze-drying and lettuce-filler addition

(Article begins on next page)
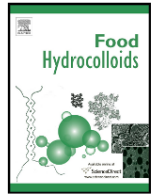
25 April 2024

Structure of oleogels from κ-carrageenan templates as affected by supercritical-CO$_2$-drying, freeze-drying and lettuce-filler addition

S. Plazzotta *, S. Calligaris , L. Manzocco

Department of Agricultural, Food, Environmental and Animal Sciences, University of Udine, Via Sondrio 2/A, 33100, Udine, Italy

ARTICLE INFO

ABSTRACT

Templates intended for food-grade oleogel production were produced by supercritical-CO$_2$-drying and freeze-drying of κ-carrageenan hydrogels (0.4 g/100 g). Supercritical-CO$_2$-drying produced hard (61 N firmness) and shrunk oleogels, which presented 80% oil content and no oil release. Freeze-drying allowed obtaining soft (2 N) oleogels, with 97% oil content but presenting a high oil release (49%). Lettuce homogenate, used as water phase of the hydrogel, acted as inactive filler agent of template network. It allowed reducing shrinkage and firmness (10 N) of supercritical-CO$_2$-dried oleogels, which presented 94% oil content and 5% oil release. In the case of freeze-dried templates, lettuce-filler increased firmness (4 N) but reduced oil release (34%). SEM image analysis highlighted that the physical properties of κ-carrageenan oleogels can be explained based on the effect of drying technique and lettuce-filler addition on the porous microstructure of the dried templates.

1. Introduction

Oleogels are self-standing systems, in which an edible liquid oil is entrapped into a tridimensional network. Oil gelation ranks among strategies for the development of fat alternatives which present enhanced nutritional value (e.g. reduced saturated fatty acid content), while maintain functionality (Martins, Vicente, Cunha, & Cerqueira, 2018). Although self-assembling lipidic compounds have been traditionally used for oil gelation, research on oil structuring using hydrophilic colloids has recently enjoyed a great deal of interest from the food sector. In this regard, different proteins and polysaccharides or their combinations have been proposed, including soy proteins, gelatine, κ-carrageenan, xanthan, hydroxypropyl methylcellulose and methylcellulose (Patel et al., 2014b; Patel, Cludts, Bin Sintang, Lesaffer, & Dewettinck, 2014; Patel et al., 2015; Tanti, Barbut, & Marangoni, 2016; Tavernier, Patel, Meeren, & Dewettinck, 2017).

The use of hydrocolloids for oil structuring is not a trivial task, due to the hydrophilic nature of these compounds, which hinders dispersion and solubilization in oil. Therefore, to achieve an oil structuring functionality, preliminary hydrocolloid gelation in a water phase is required. Water should be then removed, while preserving hydrocolloid structure as much as possible, to guarantee an efficacious oil entrapment. In this regard, Patel (2018) recently reviewed the different approaches applied to arrest the hydrocolloid structure in dried form. Among these approaches, supercritical-CO$_2$-drying has been proposed. In this case, the hydrated hydrocolloid structure is arrested in a dried template, called aerogel, which can subsequently absorb oil, leading to the final oleogel (Cassanelli, Norton, & Mills, 2017; Kocon et al., 2005b; Selmer, Kleemann, Kulozik, Heinrich, & Smirnova, 2015). Traditionally, aerogel processing starts with the formation of a gel from an aqueous solution, i.e. a hydrogel. The next step is the replacement of the water present in the gel structure by a CO$_2$-soluble solvent (alcohol) to lead to an alcoholgel. Finally, the alcohol is extracted from the gel using a continuous supercritical-CO$_2$ flow (García-González, Alnaief, & Smirnova, 2011). Being food grade, ethanol is the most used alcohol in biological applications of supercritical-CO$_2$ drying, such as the production of high-quality food products and advanced biocompatible medical devices (Brown, Fryer, Norton, & Bridson, 2010; Zambon et al., 2016). Although this technology is still mainly limited to laboratory applications, it can count on an advanced technological readiness level, which is expected to boost its commercial potentialities. Nowadays, in fact, supercritical-CO$_2$ using ethanol as co-solvent is already industrially applied to extract bioactive compounds (da Silva, Rocha-Santos, & Duarte, 2016; del Valle, 2015).

Although supercritical-CO$_2$-drying of alcoholgels allowed obtaining aerogels of tailor-made shapes and sizes from different polymers

* Corresponding author.
Email address: stella.plazzotta@uniud.it (S. Plazzotta)

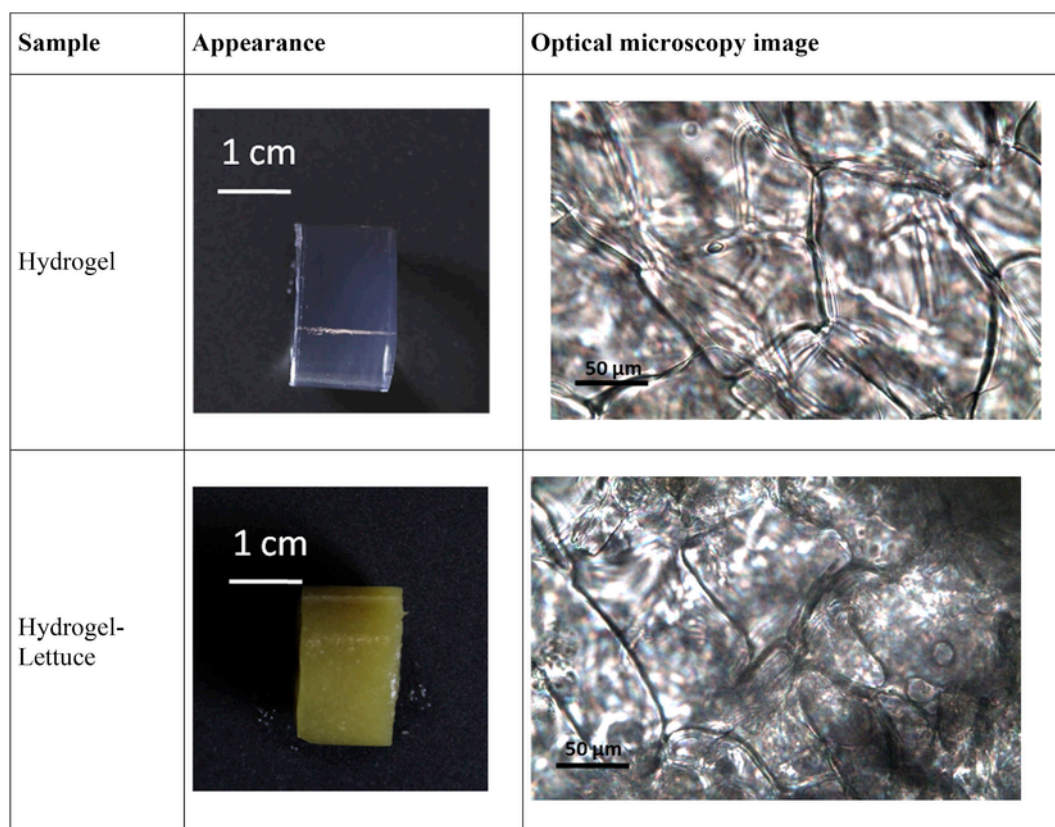| Sample	Appearance	Optical microscopy image
Hydrogel		
Hydrogel-Lettuce		

Fig. 1. Appearance and optical microscopy images of hydrogels containing κ-carrageenan (Hydrogel) or κ-carrageenan and lettuce homogenate (Hydrogel-Lettuce).

Table 1
Network density and firmness of hydrogels containing κ-carrageenan (Hydrogel) or κ-carrageenan and lettuce homogenate (Hydrogel-Lettuce).

Sample	Network density (g/cm³)	Firmness (N)
Hydrogel	0.004 ± 0.001	0.31 ± 0.07
Hydrogel-Lettuce	0.054 ± 0.002	0.35 ± 0.01

(Mikkonen, Parikka, Ghafar, & Tenkanen, 2013), it also caused extensive network shrinkage. The latter is due to the increased interactions among the polymeric chains induced by water removal (Brown et al., 2010; Comin, Temelli, & Saldaña, 2012). As a result, the obtained oleogels would have limited food applications, being characterised by a very high firmness (Manzocco et al., 2017).

To overcome this issue, both process and formulation strategies could be adopted. In particular, freeze-drying is expected to produce dried templates, called cryogels, highly retaining the original shape and volume. In fact, during this process, hydrogel water is removed by sublimation of ice crystals, which provide rigidity, limiting structural shrinkage. Nevertheless, ice crystals could crack the polymeric network, which would easily release the absorbed oil (Betz, García-González, Subrahmanyam, Smirnova, & Kulozik, 2012; Scherer, 1993). A second possibility to steer aerogel physical properties could be the modification of the hydrogel composition by the addition of filling components able to prevent the structural collapse by physically separating polymeric chains (Verdolotti, Stanzione, Khlebnikov, & Silant, 2019). In this regard, supercritical drying of lettuce has been demonstrated to lead to soft aerated materials, able to absorb huge oil amounts into a porous structure stabilised by the three-dimensional organisation of cellular tissue (Plazzotta, Calligaris, & Manzocco, 2018a; 2018b). It can be thus inferred that the addition of a lettuce filler in the template network could be exploited to control firmness of the final

dried templates, while preserving their oil absorption capacity. To this aim, lettuce waste deriving from fresh-cut processing could be used. Besides using a zero-cost raw-material, this strategy would also contribute diverting lettuce waste from traditional management options, which present high cost and elevated environmental impact (Plazzotta, Manzocco, & Nicoli, 2017).

Based on these considerations, the aim of this work was to evaluate the effect of freeze-drying, as alternative to supercritical-CO_2-drying, on the physical properties of κ-carragenan templates intended for food grade oleogel production. Moreover, the effect of the addition of a lettuce-filler was also investigated.

2. Materials and methods

2.1. Materials

κ-carrageenan was purchased from Sigma-Aldrich (Milan, Italy); potassium chloride (KCl) and sodium hypochlorite (NaClO), were purchased from Carlo Erba Reagents (Milan, Italy); absolute ethanol was purchased from J.T. Baker (Griesheim, Germany); phosphorus pentoxide (P_2O_5) was purchased from Chem-Lab NV (Zedelgem, Belgium); liquid carbon dioxide (CO_2) (purity 99.995%) was purchased from Sapio (Monza, Italy); sunflower oil was purchased in a local market (Giglio Oro, Carapelli, Firenze, Italy); *Iceberg* lettuce (*Lactuca sativa* var. *capitata*) was purchased at the local market. All solutions were prepared using milli-Q water.

2.2. Hydrogel preparation

κ-carrageenan hydrogels were prepared according to Manzocco et al. (2017). Aqueous suspensions were prepared by stirring 0.4 g/100 g κ-carrageenan and 1.0 g/100 g KCl in deionized water. κ-carragenan was

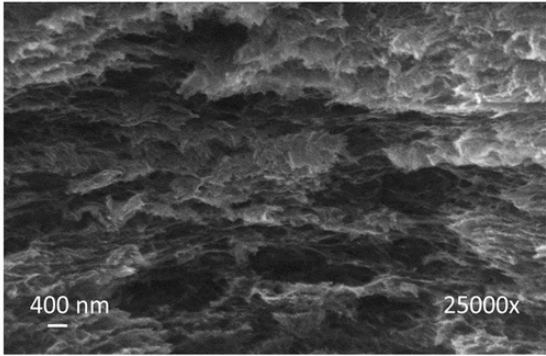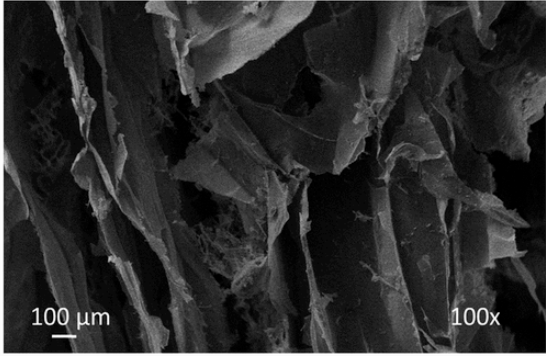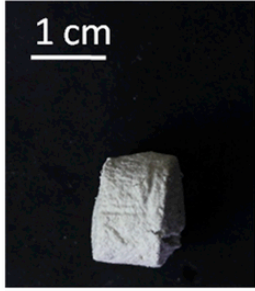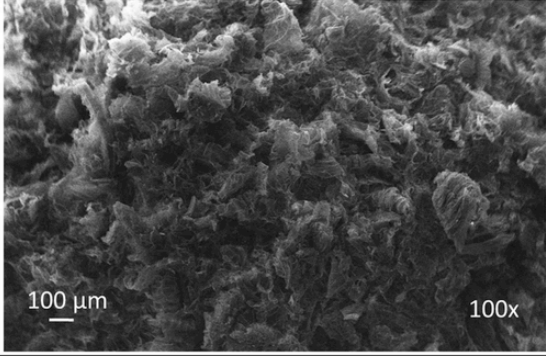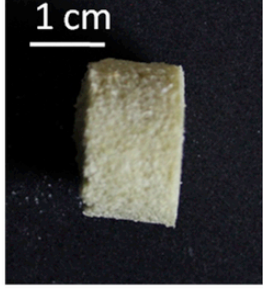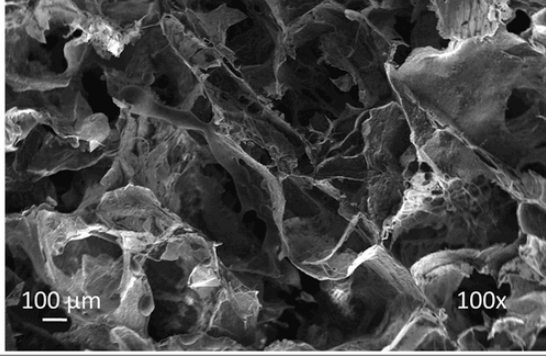| Template	Appearance	SEM micrograph
Aerogel	1 cm	400 nm 25000x
Cryogel	1 cm	100 µm 100x
Aerogel-Lettuce	1 cm	100 µm 100x
Cryogel-Lettuce	1 cm	100 µm 100x

Fig. 2. Appearance and SEM micrographs of dried templates containing κ-carrageenan (Aerogel, Cryogel) or κ-carrageenan and lettuce homogenate (Aerogel-Lettuce, Cryogel-Lettuce).

slowly added to the KCl aqueous solution at 90 °C under stirring. The homogeneous κ-carrageenan suspension was then poured into cylindrical molds of 2.5 cm diameter and 12 cm height. Hydrogel samples were cooled in an ice bath and stored for 1 day at 4 °C before analysis or further processing.

Additional hydrogels were obtained by using the same procedure above reported and substituting the deionized water with lettuce homogenate. To this purpose, a 2-kg batch of *Iceberg* lettuce was stored overnight at 4 °C. As reported in our previous work, lettuce presented the following composition (g/100 g): 94.5 humidity, 2.9 carbohydrates, 1.3 total dietary fiber, of which 92% insoluble dietary fiber, 1.1 proteins and 0.3 ashes (Plazzotta, Calligaris, & Manzocco, 2018b). Lettuce heads were treated according to Plazzotta et al. (2018b), simulating operations that are industrially carried out during fresh-cut lettuce processing. After eliminating bruised and spoiled parts, outer leaves were removed and used for the experimentation. Leaves were washed with

Table 2

Porosity, volume contraction, network density and firmness of templates containing κ-carrageenan (Aerogel, Cryogel) or κ-carrageenan and lettuce homogenate (Aerogel-Lettuce, Cryogel-Lettuce).

Template	Porosity (%)	Volume contraction (%)	Network density (g/cm^3)	Firmness (N)
Aerogel	94.3 ± 1.6 [a]	95.7 ± 0.1 [a]	0.308 ± 0.011 [a]	47.17 ± 1.87 [a]
Cryogel	95.9 ± 2.5 [a]	7.4 ± 0.2 [c]	0.004 ± 0.001 [d]	1.26 ± 0.01 [cd]
Aerogel-Lettuce	90.1 ± 1.5 [ab]	74.3 ± 0.1 [b]	0.063 ± 0.001 [b]	7.61 ± 0.66 [b]
Cryogel-Lettuce	88.2 ± 0.9 [b]	8.0 ± 0.4 [c]	0.058 ± 0.002 [c]	2.35 ± 0.17 [c]

[a-d]: in the same column, means indicated by different letters are significantly different ($p < 0.05$).

flowing water (18 ± 1 °C), sanitized 20 min in a chlorinated bath (200 mg/L of NaClO, 100 g/L leaves/water ratio), rinsed with flowing water and centrifuged in a manual kitchen centrifuge (mod. ACX01, Moulinex, France) for 1 min. To obtain the lettuce homogenate, leaves were manually chopped with a sharp knife and ground at 8000 rpm for 5 min (Polytron PT-MR3000, Kinematica AG, Littau, Switzerland).

2.3. Conversion of hydrogels into aerogels via supercritical-CO_2-drying

Before supercritical-CO_2-drying, hydrogels were converted into alcoholgels. Hydrogels were cut in cylinders with a height of about 1.5 cm and diameter of 2.5 cm and were transferred into aqueous solutions of ethanol with increasing concentrations (25, 50, 75 mL/100 mL) and maintained 1 day into each solution. Finally, samples were introduced into absolute ethanol twice (the first time for 8 h and the second one for 1 day) to remove residual water. The ratio between hydrogel and ethanol solutions was 1:8 (w/v). Conversion was carried out at room temperature (about 22 °C). Alcoholgels were converted in aerogels using the supercritical-CO_2-drying plant developed at the Department of Agricultural, Food, Environmental and Animal Sciences (University of Udine), previously described by Manzocco et al. (2017). Alcoholgels were placed inside the reactor in which CO_2 was then pressurized at 11 ± 1 MPa and 45 °C. The outlet flow through the reactor was set at 3.5 NL/min for 3 h; 5.0 NL/min for subsequent 4 h and 6.0 NL/min for subsequent 1 h. Finally, a slow decompression from 11 MPa to atmospheric pressure was carried out at 6.0 NL/min in 30 min. These flow conditions were selected since allowing drying time to be minimized while maintaining the structural integrity of the material as visually assessed.

2.4. Conversion of hydrogels into cryogels via freeze-drying

Hydrogels (40 g) were frozen at −80 °C for 24 h and then freeze-dried for 72 h at 4053 Pa by using the pilot plant model Mini Fast 1700 (Edwards Alto Vuoto, Milan, Italy).

2.5. Dried template storage

Aerogels and cryogels were stored in desiccators containing P_2O_5 at room temperature until use.

2.6. Conversion of aerogels and cryogels into oleogels via oil absorption

Aerogel and cryogel samples were introduced into 250 mL beakers previously filled with 125 mL of sunflower oil. The complete immersion of samples in the liquid phase was assured by using a plastic filter, preventing sample from floating.

2.7. Image acquisition

Images were acquired using an image acquisition cabinet (Immagini & Computer, Bareggio, Italy) equipped with a digital camera (EOS 550D, Canon, Milano, Italy). The digital camera was placed on an adjustable stand positioned 45 cm above a black cardboard base where the samples were placed. Light was provided by 4100 W frosted photographic floodlights, in a position allowing minimum shadow and glare.

2.8. Optical microscopy

Sections of hydrogel samples were placed on a glass slide, covered with a cover slide and observed at −10 °C using a Leica DM 2000 optical microscope (Leica Microsystems, Heerbrugg, Switzerland). The images were taken at 400 × magnification using a Leica EC3 digital camera and elaborated with the Leica Suite Las EZ software (Leica Microsystems, Heerbrugg, Switzerland).

2.9. Scanning electron microscopy

For scanning electron microscopy, samples were mounted on aluminium sample holders and sputter coated with 10 nm of gold using a Sputter Coater 108 auto (Cressington Scientific Instruments, Watford, United Kingdom). The aluminium holder was transferred to the SEM unit (EVO 40XVP, Carl Zeiss, Milan, Italy), which was at ambient temperature and under vacuum. Samples were imaged using an acceleration voltage of 20 kV and SmartSEM v. 5.09 (Carl Zeiss, Milan, Italy) application software was used to capture images of the samples at magnification from 100 × to 25000 × .

2.10. Volume, network density and volume contraction

Sample volume was calculated as the volume of the cylinder whose diameter and height were measured by a CD-15APXR digital caliper (Absolute AOS Digimatic, Mitutoyo Corporation, Kanagawa, Japan). Network density was calculated as the ratio between dried template weight and volume of hydrogel, aerogel, cryogel and oleogel samples. Volume changes following conversion of hydrogel to aerogel, cryogel and oleogel were expressed as the percentage ratio between the variation of sample volume and volume of the corresponding hydrogel.

2.11. Mechanical properties

Firmness was measured by uniaxial compression test using an Instron 4301 (Instron LTD., High Wycombe, UK). The instrumental settings and operations were accomplished using the software Automated Materials Testing System (version 5, Series IX, Instron LTD., High Wycombe, UK). Samples were tested using a 6.2 mm diameter cylindrical probe mounted on a 1000 N compression head at a 25 mm/min crosshead speed. Force-distance curves were obtained from the compression tests and firmness was taken as the maximum force (N) required to penetrate the sample for 5 mm.

2.12. Porosity, pore size and distribution

Porosity and pore size and distribution were estimated based on image analysis of SEM micrographs by using Image-Pro® Plus (ver. 6.3, Media Cybernetics, Inc., Bethesda, MD, USA). The center of each image was cropped to a square of 535 × 535 pixels and converted to grey-level image (8 bits). The image was binarized (conversion of the image from grey-scale to a black and white image) using an optimal threshold value (grey-level = 128), allowing the relative percentages of solid and open (pore) space to be calculated. Porosity was thus calculated as the
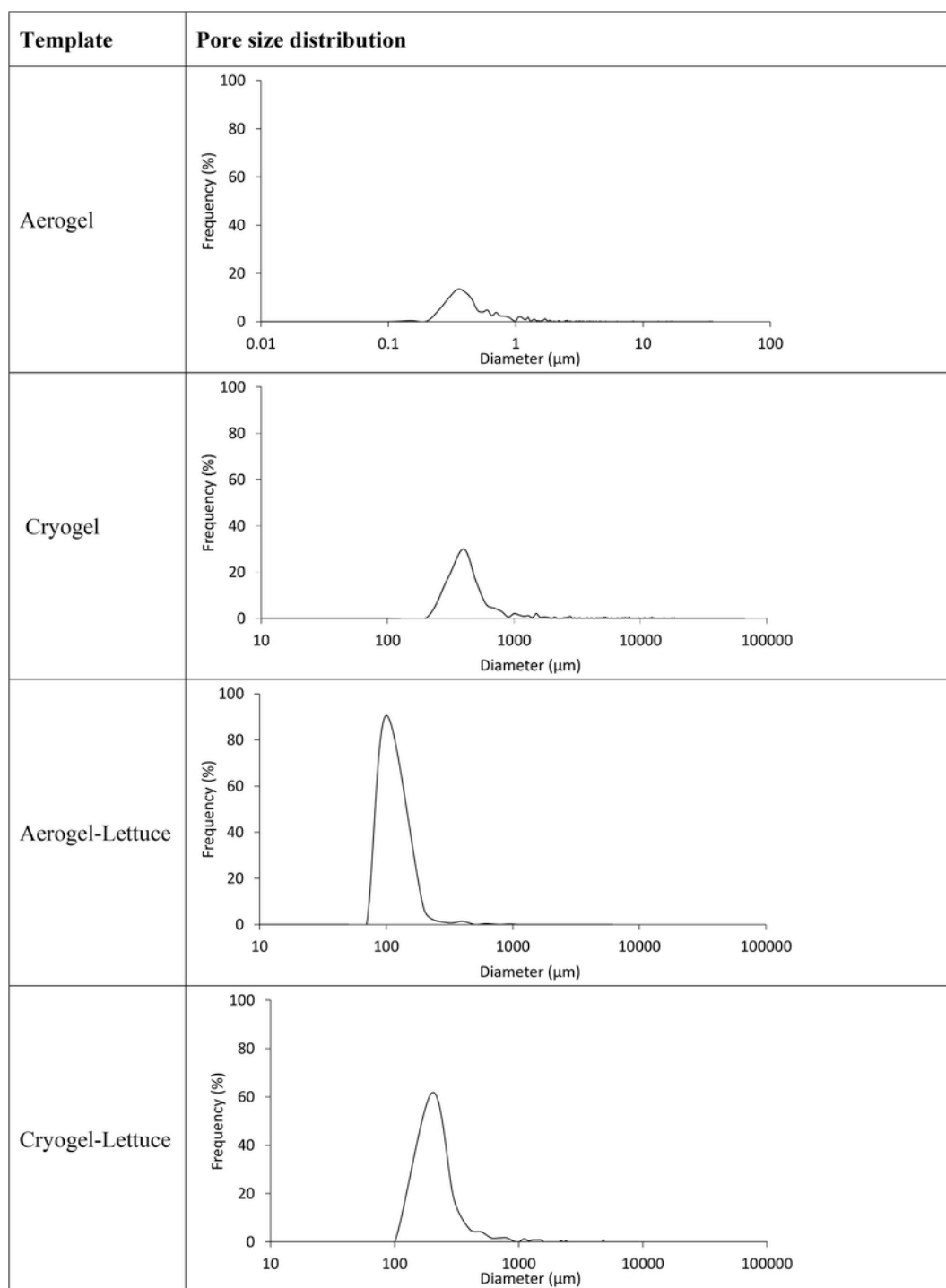
Template	Pore size distribution
Aerogel	
Cryogel	
Aerogel-Lettuce	
Cryogel-Lettuce	

Fig. 3. Frequency distributions of pore dimensions of templates containing κ-carrageenan (Aerogel, Cryogel) or κ-carrageenan and lettuce homogenate (Aerogel-Lettuce, Cryogel-Lettuce).

percentage ratio between the total area corresponding to pores and the overall sum of image pixels. Pores were automatically recognised as objects having grey-level beyond the selected threshold. The maximal diameter (in pixels) of pores was estimated by the program and converted in metric units by comparison with a 400 nm or 100 μm scale. Acquired data were subsequently elaborated to obtain pore size frequency distributions (Microsoft® Excel 2016).

2.13. FTIR measurement

Spectra were recorded at $25 \pm 1\,°C$ by using a FTIR instrument, equipped with an ATR accessory and a Zn–Se crystal that allows collection of FTIR spectra directly on sample without any special preparation (Alpha-P, Bruker Optics, Milan, Italy). The "pressure arm" of the in-instrument was used to apply constant pressure to the samples positioned on the top of the Zn–Se crystal, to ensure a good contact be-
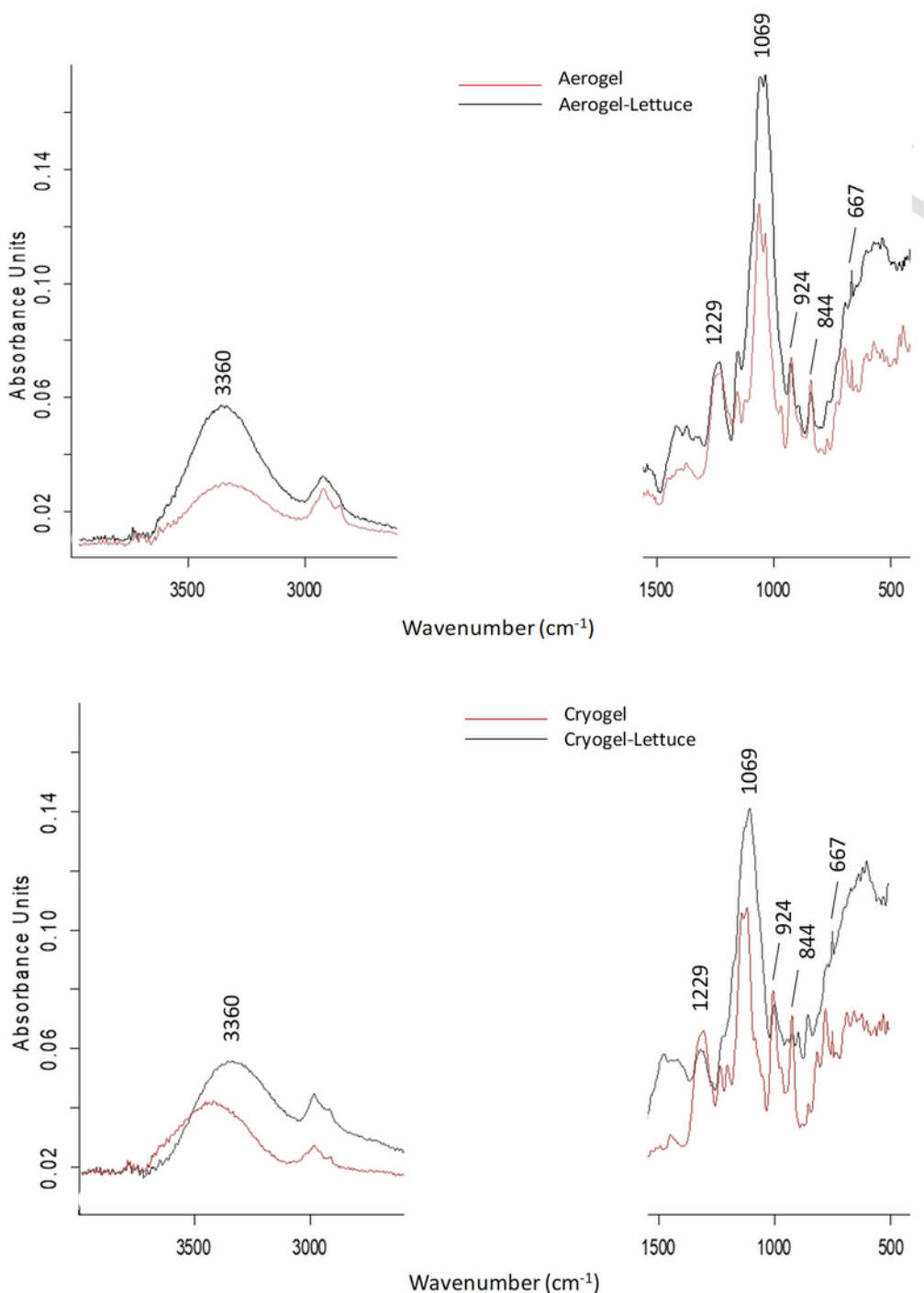
Fig. 4. FTIR spectra of templates containing κ-carrageenan (Aerogel, Cryogel) or κ-carrageenan and lettuce homogenate (Aerogel-Lettuce, Cryogel-Lettuce).

tween the sample and the incident IR beam. All FTIR spectra were collected in the range from 4000 to 400 cm^{-1}, at a spectrum resolution of 4 cm^{-1} and with 32 co-added scans. Background scan of the clean Zn–Se crystal was acquired prior to sample scanning.

2.14. Oil absorption kinetics and oil content

At defined time intervals during conversion from aerogel or cryogel to oleogel (paragraph 2.6), samples were withdrawn, wiped with absorbing paper and weighted. Absorbed oil was determined based on the weight gain at time *t*. Absorbed oil was calculated as the ratio between weight gain at time *t* and the weight of the aerogel/cryogel. Oil absorption kinetic data were fitted using the oil absorbing model reported in eq. (1) (Khosravi & Azizian, 2016).

$$y_t = y_{max}(1 - e^{-\beta t}) \tag{1}$$

where y_t is the oil absorbed at time *t*, y_{max} is the maximum amount of absorbed oil, β (min^{-1}) is the apparent mass transfer coefficient, proportional to apparent diffusion coefficient of oil into the pores. The immersion of aerogel or cryogel into oil was prolonged until a constant weight after two consequent readings was reached (*plateau* value). Oil content of oleogels was defined as the percentage ratio between the amount of oil at the absorption *plateau* value and the oleogel weight.
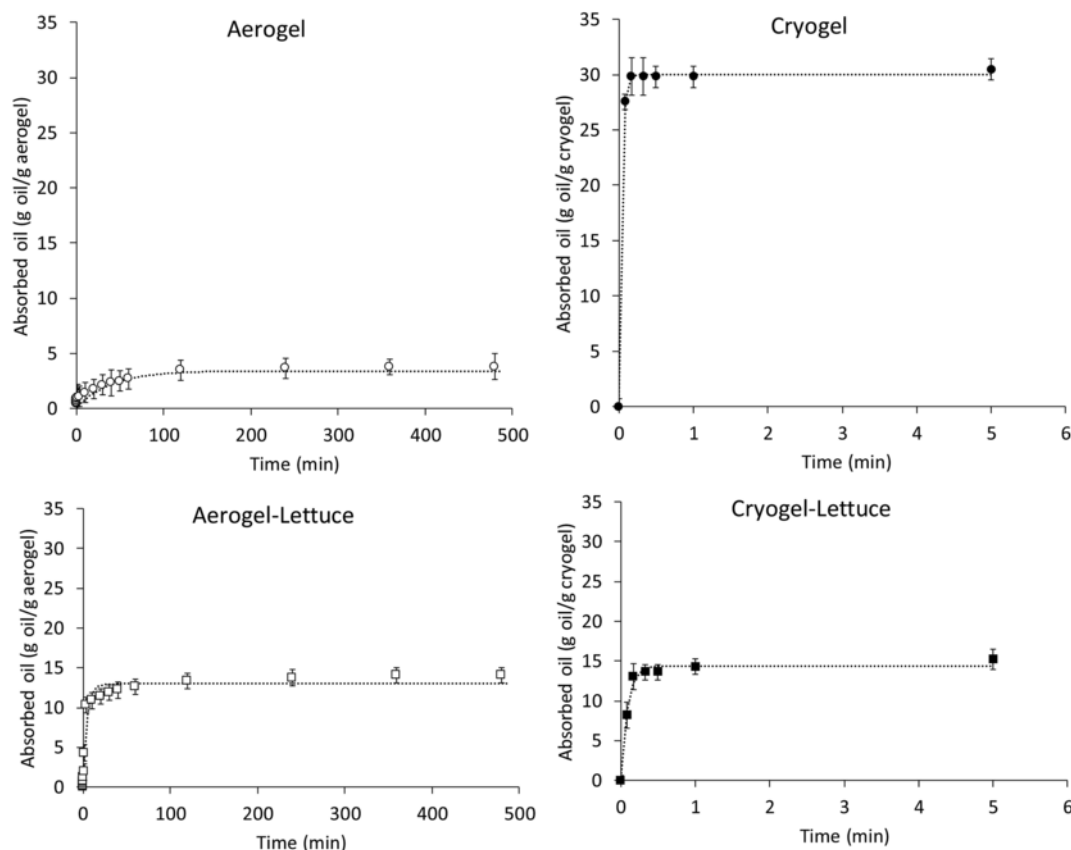
Fig. 5. Oil absorbed by templates containing κ-carrageenan (Aerogel, Cryogel) or κ-carrageenan and lettuce homogenate (Aerogel-Lettuce, Cryogel-Lettuce) as a function of time (symbols). Fitting curves of oil absorption model are also reported (dotted lines).

Table 3

Model parameter estimates for oil absorption into templates containing κ-carrageenan (Aerogel, Cryogel) or κ-carrageenan and lettuce homogenate (Aerogel-Lettuce, Cryogel-Lettuce).

Template	y_{max} (g oil/g cryogel or aerogel)	β (min^{-1})	R^2
Aerogel	3.41	0.03	0.891
Cryogel	29.99	30.18	0.999
Aerogel-Lettuce	12.98	0.21	0.966
Cryogel-Lettuce	14.37	11.24	0.986

Table 4

Oil content, volume contraction, network density and firmness of oleogels obtained from templates containing κ-carrageenan (Aerogel, Cryogel) or κ-carrageenan and lettuce homogenate (Aerogel-Lettuce, Cryogel-Lettuce).

Oleogel template	Oil content (%, w/w)	Volume contraction (%)	Network density (g/cm^3)	Firmness (N)
Aerogel	79.5 ± 0.3 [c]	98.9 ± 0.1 [a]	0.413 ± 0.011 [a]	61.24 ± 3.43 [a]
Cryogel	96.8 ± 0.2 [a]	10.3 ± 0.4 [c]	0.005 ± 0.001 [c]	1.70 ± 0.01 [c]
Aerogel-Lettuce	94.0 ± 0.6 [b]	74.2 ± 0.9 [b]	0.065 ± 0.001 [b]	9.60 ± 1.05 [b]
Cryogel-Lettuce	94.7 ± 0.5 [b]	11.4 ± 0.5 [c]	0.020 ± 0.001 [c]	3.79 ± 0.34 [bc]

[a-c]: in the same column, means indicated by different letters are significantly different ($p < 0.05$).
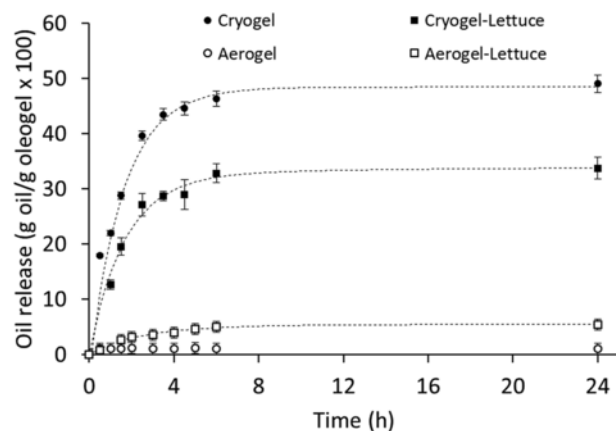
Fig. 6. Oil release from oleogels obtained from templates containing κ-carrageenan (Aerogel, Cryogel) or κ-carrageenan and lettuce homogenate (Aerogel-Lettuce, Cryogel-Lettuce) as a function of time (symbols). Fitting curves of oil desorption model are also reported (dotted lines).

2.15. Oil desorption kinetics

Oil desorption measurements were carried out using the method of Blake, Co, and Marangoni (2014) with some modifications. Oleogel samples (2 g) were positioned on accurately weighted Whatman # 5 filter paper (125 mm diameter). The amount of lost oil was determined by accurately weighting oleogels at defined time intervals up to 24 h and expressed as percentage ratio of lost oil and oleogel initial weight. Data were fitted using a two-phase exponential decay model (Blake et

Table 5

Model parameter estimates for oil released by oleogels obtained from templates containing κ-carrageenan (Cryogel) or κ-carrageenan and lettuce homogenate (Aerogel-Lettuce, Cryogel-Lettuce).

Oleogel template	Fast component		Slow component		y_{max} (%)	R^2
	y_{fast} (%)	k_{fast} (min^{-1})	y_{slow} (%)	k_{slow} (min^{-1})		
Cryogel	37.05	0.014	11.99	0.005	49.04	0.990
Aerogel-Lettuce	4.25	0.005	1.18	0.013	5.43	0.992
Cryogel-Lettuce	16.48	0.009	17.05	0.009	33.53	0.989

al., 2014) (eq. (2)).

$$y = y_{fast}(1 - e^{(-k_{fast}t)}) + y_{slow}(1 - e^{(-k_{slow}t)}) \qquad (2)$$

$$y_{max} = y_{fast} + y_{slow} \qquad (3)$$

where y_{fast} and y_{slow} are the asymptote values of the fast- and slow-decaying components, respectively, k_{fast} and k_{slow} are the rate constants for the fast- and slow-decaying component, respectively, and y_{max} is the maximum amount of lost oil when time t tends to infinite and is the sum of y_{fast} and y_{slow} (eq. (3)).

2.16. Data analysis

All determinations were expressed as the mean ± standard error of at least three repeated measurements from two experiment replicates. Statistical analysis was performed by using R v. 3.0.2 (The R foundation for Statistical Computing). Bartlett's test was used to check the homogeneity of variance. One-way ANOVA was carried out and Tukey-test was used as post-hoc test to determine statistically significant differences among means ($p < 0.05$). Non-linear regression analysis of absorbed and desorbed oil as a function of time was performed by using TableCurve2D software (Jandel Scientific, ver. 5.01). The goodness of fit was evaluated based on statistical parameters of fitting (R^2, p) and the residual analysis.

3. Results and discussion

3.1. Effect of drying process on κ-carrageenan templates

κ-carrageenan Hydrogel was obtained using the gelling capacity of this polymer, which forms random coils transiting to a double helix conformation in the presence of potassium monovalent ions (K^+) (Rinaudo, 2008) (Fig. 1). The microscopic image of the Hydrogel revealed that water was efficaciously entrapped in the κ-carrageenan network, organized in pouches of about 100–200 μm (Fig. 1). Additional samples were prepared by substituting the aqueous phase of the κ-carrageenan hydrogel with lettuce homogenate (Hydrogel-Lettuce sample). The presence of lettuce did not impair κ-carrageenan gelling ability but resulted in a more crowded microstructure, in which the network pouches were filled with vegetable material dispersed in the aqueous phase (Fig. 1). This suggests that lettuce mainly acted as inactive filling agent of the polymeric network. Lettuce addition also increased hydrogel density ($p < 0.05$) (Table 1), due to the fact that lettuce homogenate contains about 5% dry matter (paragraph 2.2). In particular, insoluble fiber, representing about 20% of lettuce dry weight, is expected to highly contribute to the structural architecture of the sample, being retained within the network and not solubilised in the water phase. Noteworthily, lettuce homogenate addition did not

significantly affect hydrogel firmness ($p \geq 0.05$, Table 1), supporting the hypothesis that lettuce mainly acted as inactive filler of the network voids, without altering its interactions.

Hydrogel samples were subjected to supercritical-CO_2-drying and freeze-drying leading to the dried templates called Aerogel and Cryogel. The appearance of κ-carrageenan Aerogel and Cryogel are reported in Fig. 2. Differently from the Hydrogel, which appeared transparent, both templates resulted completely opaque, suggesting that drying led to a porous structure, promoting an intense scattering of incident light (Alince & Lepoutre, 1980; Betz et al., 2012; Manzocco et al., 2017). In order to confirm this hypothesis, the dried template structure was observed using SEM (Fig. 2). As it can be seen from the SEM image at 100 × magnification (Supplementary Fig. S1), the Aerogel obtained via supercritical-drying, showed a strongly contracted structure, in agreement with previous studies exploiting biopolymers such as κ-carrageenan and β-glucan to produce aerogels (Comin et al., 2012; Manzocco et al., 2017). During supercritical drying, water is replaced, reducing the number of hydrogen bonds between the κ-carrageenan chains and the water molecules, while favouring the interactions between individual polymeric strands. This increase in intermolecular polymer junction zones results in strong structure contraction (Comin et al., 2012). The porous structure was only visible at 25000 × magnification (Fig. 2) and the porosity of the Aerogel resulted higher than 94% (Table 2), with 20% of pores presenting a mean dimension of 400 nm but with smaller and larger-dimension tails ranging from 200 nm up to 1 μm (Fig. 3). By contrast, a light aerated Cryogel, presenting a porosity higher than 95% was obtained via freeze-drying (Fig. 2, Table 2). Cryogel pore size ranged from 200 up to 900 μm (Fig. 3), resulting higher than that of the water pouches originally present in the hydrogel (Fig. 1). This suggests that freeze-drying promoted the local displacement of κ-carrageenan polymeric chains, possibly due to the formation and growth of ice crystals during freezing. Subsequently, the sublimation of ice crystals resulted in a ballooning effect and thus in the formation of large pores (Betz et al., 2012; Kocon, Job, & The, 2005a).

The presence of lettuce deeply altered template microstructure (Fig. 2). Aerogel-Lettuce and Cryogel-Lettuce presented a highly homogeneous structure, with respectively 90 and 60% of the pores having a mean dimension of about 100 and 200 μm, respectively (Fig. 3), comparable to that of the initial hydrogel (Fig. 1). This supports the hypothesis that lettuce acted as a filling agent able to contain template shrinkage during supercritical-CO_2-drying or to fill template voids left upon freeze-drying. Lettuce also increased template crowding, resulting in a 4 and 8% porosity reduction as compared to Aerogel and Cryogel, respectively (Table 2).

To investigate the effect of these different microstructures on the physical properties of the dried templates, the latter were analyzed for volume contraction, network density and firmness (Table 2). As a result of the severe volume shrinkage, Aerogel network density and firmness resulted extremely higher than those of the initial Hydrogel (Table 1). By contrast, the Cryogel showed a slight volume contraction, mostly retaining the Hydrogel network density. This can be attributed to the fact that ice crystals maintained the structural rigidity of the material during drying (Betz et al., 2012; Ratti, 2001). Consequently, the κ-carrageenan Cryogel resulted almost 40 times softer than the Aerogel (Table 2). Aerogel-Lettuce showed firmness and network density lower than those of the corresponding Aerogel. By contrast, Cryogel-Lettuce presented firmness and network density higher than those obtained without lettuce, despite the similar volume contraction. The final template density and firmness are thus the result of two counteracting effects: the increase of dry matter upon lettuce addition and the decrease of volume contraction. The latter prevailed over the former in the case of the Aerogel-Lettuce, resulting in a network density and firmness lower than those observed in the Aerogel. By contrast, in the case of

Cryogel-Lettuce, the dry-matter effect prevailed, leading to network density and firmness higher than those observed in the absence of lettuce (Table 2).

FTIR analysis was also used to study the fundamentals vibrations of chemical groups in the systems (Fig. 4). Aerogel and Cryogel samples gave the typical spectrum of κ-carrageenan, which presents a broad band in the IR region from 3700 to 3000 cm^{-1} and lower intensity peaks at 1229, 1069, 924 and 844 cm^{-1}. These peaks can be attributed to OH-stretching vibrations arising from hydrogen bonding, sulphate ester, glycosidic linkage, 3,6-anhydro-D-galactose and D-galactose-4-sulphate, respectively (Manuhara, Praseptiangga, & Riyanto, 2016). As expected, lettuce addition altered the FTIR spectra of the dried templates, modifying the fingerprint κ-carrageenan band at 1069 cm^{-1} and increasing the intensity of the band at 3700 to 3000 cm^{-1} and of the peak at 667 cm^{-1}, which have been associated to –OH vibrations typical of cellulose hydrogen bonding (Abid, Cabrales, & Haigler, 2014). Nevertheless, Aerogel-Lettuce and Cryogel-Lettuce gave similar spectra (Fig. 4), confirming that the drying technique did not alter the fundamental groups of the template constituents.

3.2. Oleogel preparation from dried templates

The potentialities of κ-carrageenan templates to be used for oleogel preparation was evaluated by immersion into sunflower oil. All samples progressively absorbed oil until reaching a *plateau* value (Fig. 5). Data were fitted with the model proposed by Khosravi and Azizian (2016) for oil absorption into porous materials. The selected model neatly fitted data, leading to R^2 values reported in Table 3. The parameter y_{max} of the absorption model estimates the maximum oil absorption capacity, while β is proportional to the oil apparent diffusion coefficient into the template. The Cryogel presented y_{max} and β parameters much higher than those of the Aerogel, indicating that the κ-carrageenan templates obtained via freeze-drying absorbed a higher oil amount in much shorter time (5 min) as compared to supercritical-dried ones (8 h) (Fig. 5). This can be traced back to the strongly contracted microstructure of Aerogel, which would absorb oil more slowly than the large pores of Cryogel (Fig. 2).

Lettuce addition significantly affected the oil absorption ability of the templates (Fig. 5). Aerogel-Lettuce showed values of both β and y_{max} higher than those of Aerogel, while the opposite was observed in the case of Cryogel-Lettuce (Table 3). These contrasting results can be explained in the light of the effect of lettuce addition on Aerogel and Cryogel structure. In the first case, lettuce-filler physically hindered structural shrinkage (Table 2), resulting in a template with larger pores (Figs. 2 and 3), able to absorb a higher oil amount (Fig. 5). In the second case, lettuce acted as a filler of the large pores obtained upon freeze-drying (Figs. 2 and 3), reducing the volume available for oil absorption (Fig. 5). Noteworthily, upon oil absorption, the templates maintained their integrity, leading to oleogels with the physical properties shown in Table 4. The oil content of oleogels resulted particularly high and affected by the overall volume contraction of the template. In particular, the shrunk Aerogel absorbed an oil amount significantly lower than that of the not-contracted Cryogel. Due to the lower volume contraction, Aerogel-Lettuce template turned into an oleogel presenting an oil content significantly higher than that of the oleogel without lettuce homogenate, as well as a considerably lower firmness (Table 4). By contrast, in the templates obtained upon freeze-drying, lettuce reduced pore volume available for oil absorption. In all samples, oil absorption caused only a slight further contraction of template volume (Table 4) as compared to the one induced by the drying step (Table 2). Consequently, minor increase in network density and firmness was detected upon oil loading into the dried templates (Table 4). This suggests that oil slightly interacted with template constituents and did not significantly alter the tridimensional architecture of κ-car-

rageenan network. Based on this observation, it could be inferred that oil absorption in the templates is mainly driven by capillary forces, with minor involvement of chemical interactions.

To better investigate oleogel properties, oil desorption kinetics were determined by monitoring the oil amount lost by oleogels during a 24-h storage (Fig. 6). Kinetics of oil release were fitted with the two-phase decay exponential model proposed by Blake et al. (2014) for analysing oil desorption from oleogels. The oleogel obtained from the Aerogel resulted particularly stable, presenting an oil release lower than 1% (w/w). For this reason, oil desorption modelling was not performed on data relevant to this sample. By contrast, the oleogel obtained from the other templates progressively released oil, allowing a good model fitting of experimental data, as shown by R^2 value reported in Table 5. The model posits that the oil absorbed into an oleogel includes two different fractions: (i) oil weakly entrapped in the network, which is fast released; (ii) oil strongly adsorbed onto the network surface, which is slowly desorbed. Therefore, the model consists of a fast and a slow component. Within one day of storage, the oleogel obtained from the Cryogel lost a considerable oil amount (about 50%, y_{max}), which was mainly desorbed according to a fast kinetics (about 37%, y_{fast}). This suggests that oil was only weakly entrapped in the Cryogel, probably due to its large-pore structure (Figs. 2 and 3), which would fast absorb oil, without being able to hold it. As anticipated, the oleogel deriving from the Aerogel showed no significant oil release. Presenting pores of smaller size (Figs. 2 and 3), the Aerogel would slowly absorb a lower oil amount as compared to the Cryogel (Fig. 5) but would highly retain it into the small-size pore structure. When lettuce was added (Aerogel-Lettuce), a small amount of the absorbed oil was lost (y_{max}, Table 5). This suggests that lettuce addition reduced the surface available for oil holding by increasing pore size (Figs. 2 and 3). By contrast, oil released from the Cryogel-Lettuce template resulted considerably lower than that released by the Cryogel (y_{max}, Table 5). In this case, in fact, lettuce filled the large template pores (Figs. 2 and 3), leading to an increase of the surface available for oil binding, as highlighted by the increase of the parameters related to the slow model component (Table 5).

4. Conclusions

Both processing and formulation strategies can be used to steer the physical properties of κ-carrageenan templates intended for edible oleogel production. The use of supercritical-CO$_2$-drying allows obtaining stable oleogels, whose high firmness, however, would limit their food use. On the opposite, freeze-drying allows obtaining soft oleogels which, however, easily release oil. The addition of lettuce homogenate deriving from fresh-cut processing waste can cheaply overcome these issues, acting as an inactive filler able to prevent polymeric chains packing during supercritical-CO$_2$-drying and large pore formation during freeze-drying.

Results here presented are relevant to the specific case of κ-carrageenan templates but the proposed strategies could be definitely extended to other food-grade hydrocolloids with gelling properties, greatly enhancing the possibility to develop novel oleogels with tailored physical properties.

Appendix A. Supplementary data

Supplementary data to this article can be found online at https://doi.org/10.1016/j.foodhyd.2019.05.008.

References

Abid, N., Cabrales, L., Haigler, C.H., 2014. Changes in the cell wall and cellulose content of developing cotton fibres investigated by FTIR spectroscopy. Charbohydrate Polymers 100, 9–16.

Alince, B., Lepoutre, P., 1980. Porosity and optical properties of clay coatings. Journal of Colloid and Interface Science 76, 439–444.

Betz, M., García-González, C.A., Subrahmanyam, R.P., Smirnova, I., Kulozik, U., 2012. Preparation of novel whey protein-based aerogels as drug carriers for life science applications. The Journal of Supercritical Fluids 72, 111–119.

Blake, A.I., Co, E.D., Marangoni, A.G., 2014. Structure and physical properties of plant wax crystal networks and their relationship to oil binding capacity. JAOCS, Journal of the American Oil Chemists' Society 91, 885–903.

Brown, Z.K., Fryer, P.J., Norton, I.T., Bridson, R.H., 2010. Drying of agar gels using supercritical carbon dioxide. The Journal of Supercritical Fluids 54, 89–95.

Cassanelli, M., Norton, I., Mills, T., 2017. Effect of alcohols on gellan gum gel structure: Bridging the molecular level and the three-dimensional network. Food Structure 14, 112–120.

Comin, L.M., Temelli, F., Saldaña, M.D.A., 2012. Barley beta-glucan aerogels via supercritical CO_2 drying. Food Research International 48, 442–448.

García-González, C.A., Alnaief, M., Smirnova, I., 2011. Polysaccharide-based aerogels-Promising biodegradable carriers for drug delivery systems. Carbohydrate Polymers 86, 1425–1438.

Khosravi, M., Azizian, S., 2016. A new kinetic model for absorption of oil spill by porous materials. Microporous and Mesoporous Materials 230, 25–29.

Kocon, L., Job, N., The, A., 2005a. Carbon aerogels, cryogels and xerogels: Influence of the drying method on the textural properties of porous carbon materials. Carbon 43, 2481–2494.

Kocon, L., Job, N., The, A., Théry, A., Pirard, R., Marien, J., et al., 2005b. Carbon aerogels, cryogels and xerogels: Influence of the drying method on the textural properties of porous carbon materials. Carbon 43, 2481–2494.

Manuhara, G.J., Praseptiangga, D., Riyanto, R.A., 2016. Extraction and characterization of refined κ-carrageenan of red algae [kappaphycus alvarezii (doty ex P.C. Silva, 1996)] originated from karimun jawa islands. Aquatic Procedia 7, 106–111.

Manzocco, L., Valoppi, F., Calligaris, S., Andreatta, F., Spilimbergo, S., Nicoli, M.C., 2017. Exploitation of κ-carrageenan aerogels as template for edible oleogel preparation. Food Hydrocolloids 71, 68–75.

Martins, A.J., Vicente, A.A., Cunha, R.L., Cerqueira, M.A., 2018. Edible oleogels: An opportunity for fat replacement in foods. Food and Function

Mikkonen, K.S., Parikka, K., Ghafar, A., Tenkanen, M., 2013. Prospects of polysaccharide aerogels as modern advanced food materials. Trends in Food Science & Technology 34, 124–136.

Patel, A.R., 2018. Structuring edible oils with hydrocolloids: Where do we stand?. Food Biophysics 13, 113–115.

Patel, A.R., Cludts, N., Bin Sintang, M.D., Lesaffer, A., Dewettinck, K., 2014a. Edible oleogels based on water soluble food polymers: Preparation, characterization and potential application. Food & Function 5, 2833–2841.

Patel, A.R., Cludts, N., Bin Sintang, M.D., Lewille, B., Lesaffer, A., Dewettinck, K., 2014b. Polysaccharide-based oleogels prepared with an emulsion-templated approach. ChemPhysChem 15, 3435–3439.

Patel, A.R., Rajarethinem, P.S., Cludts, N., Lewille, B., De Vos, W.H., Lesaffer, A., et al., 2015. Biopolymer-based structuring of liquid oil into soft solids and oleogels using water-continuous emulsions as templates. Langmuir 31, 2065–2073.

Plazzotta, S., Calligaris, S., Manzocco, L., 2018a. Application of different drying techniques to fresh-cut salad waste to obtain food ingredients rich in antioxidants and with high solvent loading capacity. Lebensmittel-Wissenschaft und -Technologie- Food Science and Technology 89, 276–283.

Plazzotta, S., Calligaris, S., Manzocco, L., 2018b. Innovative bioaerogel-like materials from fresh-cut salad waste via supercritical-CO_2-drying. Innovative Food Science & Emerging Technologies 47, 485–492.

Plazzotta, S., Manzocco, L., Nicoli, M.C., 2017. Fruit and vegetable waste management and the challenge of fresh-cut salad. Trends in Food Science & Technology 63, 51–59.

Ratti, C., 2001. Hot air and freeze-drying of high-value foods: A review. Journal of Food Engineering 49, 311–319.

Rinaudo, M., 2008. Main properties and current applications of some polysaccharides as biomaterials. Polymer International 430, 397–430.

Scherer, G.W., 1993. Freezing gels. Journal of Non-crystalline Solids 155, 1–25.

Selmer, I., Kleemann, C., Kulozik, U., Heinrich, S., Smirnova, I., 2015. Development of egg white protein aerogels as new matrix material for microencapsulation in food. The Journal of Supercritical Fluids 106, 42–49.

da Silva, R.P.F.F., Rocha-Santos, T.A.P., Duarte, A.C., 2016. Supercritical fluid extraction of bioactive compounds. Trends in Analytical Chemistry 76, 40–51.

Tanti, R., Barbut, S., Marangoni, A.G., 2016. Hydroxypropyl methylcellulose and methylcellulose structured oil as a replacement for shortening in sandwich cookie creams. Food Hydrocolloids 61, 329–337.

Tavernier, I., Patel, A.R., Meeren, P. Van Der, Dewettinck, K., 2017. Emulsion-templated liquid oil structuring with soy protein and soy protein: k -carrageenan complexes. Food Hydrocolloids 65, 107–120.

del Valle, J.M., 2015. Extraction of natural compounds using supercritical CO_2: Going from the laboratory to the industrial application. The Journal of Supercritical Fluids 96, 180–199.

Verdolotti, L., Stanzione, M., Khlebnikov, O., Silant, V., 2019. Dimensionally stable cellulose aerogel strengthened by polyurethane synthesized in situ. Macromolecular Chemistry and Physics 1–10, 1800372.

Zambon, A., Vetralla, M., Urbani, L., Pantano, M.F., Ferrentino, G., Pozzobon, M., et al., 2016. Dry acellular oesophageal matrix prepared by supercritical carbon dioxide. The Journal of Supercritical Fluids 115, 33–41.